Landscape of somatic mutations and clonal evolution in mantle cell lymphoma

Sílvia Beà[a,1], Rafael Valdés-Mas[b], Alba Navarro[a], Itziar Salaverria[a], David Martín-Garcia[a], Pedro Jares[a], Eva Giné[a], Magda Pinyol[a], Cristina Royo[a], Ferran Nadeu[a], Laura Conde[a], Manel Juan[a], Guillem Clot[a], Pedro Vizán[c], Luciano Di Croce[c], Diana A. Puente[b], Mónica López-Guerra[a], Alexandra Moros[a], Gael Roue[a], Marta Aymerich[a], Neus Villamor[a], Lluís Colomo[a], Antonio Martínez[a], Alexandra Valera[a], José I. Martín-Subero[a], Virginia Amador[a], Luis Hernández[a], Maria Rozman[a], Anna Enjuanes[a], Pilar Forcada[d], Ana Muntañola[d], Elena M. Hartmann[e], María J. Calasanz[f], Andreas Rosenwald[e], German Ott[g], Jesús M. Hernández-Rivas[h], Wolfram Klapper[i], Reiner Siebert[j], Adrian Wiestner[k], Wyndham H. Wilson[l], Dolors Colomer[a], Armando López-Guillermo[a], Carlos López-Otín[b,2], Xose S. Puente[b,1,2], and Elías Campo[a,1,2]

[a]Institut d'Investigacions Biomèdiques August Pi i Sunyer, Hospital Clínic, Universitat de Barcelona, 08036 Barcelona, Spain; [b]Instituto Universitario de Oncología, Universidad de Oviedo, 33006 Oviedo, Spain; [c]Center for Genomic Regulation and Universitat Pompeu Fabra, 08003 Barcelona, Spain; [d]Mutua de Terrassa, 08221 Terrassa, Spain; [e]Institute of Pathology, University of Würzburg, 97080 Würzburg, Germany; [f]Departamento de Genética, Universidad de Navarra, 31080 Pamplona, Spain; [g]Robert-Bosch-Krankenhaus and Dr. Margarete Fischer-Bosch Institute of Clinical Pharmacology, 70376 Stuttgart, Germany; [h]Centro de Investigación del Cáncer, Universidad de Salamanca, 37007 Salamanca, Spain; [i]Hematopathology Section and Lymph Node Registry, University of Kiel, D-24105 Kiel, Germany; [j]Institute of Human Genetics, University of Kiel, D-24105 Kiel, Germany; [k]National Heart, Lung, and Blood Institute, Bethesda, MD 20892; and [l]National Cancer Institute, Bethesda, MD 20892

Edited* by Louis M. Staudt, National Institutes of Health, Bethesda, MD, and approved September 19, 2013 (received for review August 7, 2013)

Mantle cell lymphoma (MCL) is an aggressive tumor, but a subset of patients may follow an indolent clinical course. To understand the mechanisms underlying this biological heterogeneity, we performed whole-genome and/or whole-exome sequencing on 29 MCL cases and their respective matched normal DNA, as well as 6 MCL cell lines. Recurrently mutated genes were investigated by targeted sequencing in an independent cohort of 172 MCL patients. We identified 25 significantly mutated genes, including known drivers such as ataxia-telangectasia mutated (*ATM*), cyclin D1 (*CCND1*), and the tumor suppressor *TP53*; mutated genes encoding the anti-apoptotic protein *BIRC3* and Toll-like receptor 2 (*TLR2*); and the chromatin modifiers *WHSC1*, *MLL2*, and *MEF2B*. We also found *NOTCH2* mutations as an alternative phenomenon to *NOTCH1* mutations in aggressive tumors with a dismal prognosis. Analysis of two simultaneous or subsequent MCL samples by whole-genome/whole-exome ($n = 8$) or targeted ($n = 19$) sequencing revealed subclonal heterogeneity at diagnosis in samples from different topographic sites and modulation of the initial mutational profile at the progression of the disease. Some mutations were predominantly clonal or subclonal, indicating an early or late event in tumor evolution, respectively. Our study identifies molecular mechanisms contributing to MCL pathogenesis and offers potential targets for therapeutic intervention.

next-generation sequencing | cancer genetics | cancer heterogeneity

Mantle cell lymphoma (MCL) is a mature B-cell neoplasm characterized by the t(11;14)(q13;q32) translocation leading to the overexpression of cyclin D1 (1). *CCND1* is a weak oncogene that requires the cooperation of other oncogenic events to transform lymphoid cells (2). Molecular studies have identified alterations in components of the cell-cycle regulation, DNA damage response, and cell survival pathways (3, 4), but the profile of mutated genes contributing to the pathogenesis of MCL and cooperating with *CCND1* is not well defined (1). Most MCL cases have a rapid evolution and an aggressive behavior with an unfavorable outcome with current therapies (5). Paradoxically, a subset of patients follows an indolent clinical evolution with stable disease even in the absence of chemotherapy (6, 7). This favorable behavior has been associated with *IGHV*-mutated (8, 9) and lack of expression of *SOX11* (10, 11), a transcription factor highly specific of MCL that contributes to the aggressive behavior of this tumor (12). However, the molecular mechanisms responsible for this clinical heterogeneity are not well understood.

To gain insight into the molecular pathogenesis of MCL we performed whole-genome sequencing (WGS) and whole-exome sequencing (WES) of 29 MCL and further investigated mutated genes in an expanded series of patients. We also analyzed the subclonal heterogeneity of the tumors and their modulation during the evolution of the disease.

Results

Landscape of Mutations in MCL. We performed WGS and WES of 4 and 29 MCL, respectively. These patients were representative of the broad clinical and biological spectrum of the disease, including five patients with an indolent clinical evolution. In

Significance

This is a comprehensive whole-genome/whole-exome analysis of mantle cell lymphoma (MCL). We sequenced 29 MCL cases and validated the findings by target sequencing of 172 additional tumors. We identified recurrent mutations in genes regulating chromatin modification and genes such as *NOTCH2* that have a major impact on clinical outcome. Additionally, we demonstrated the subclonal heterogeneity of the tumors already at diagnosis and the modulation of the mutational architecture in the progression of the disease. The identification of new molecular mechanisms may open perspectives for the management of MCL patients.

Author contributions: S.B., C.L.-O., X.S.P., and E.C. designed research; S.B., R.V.-M., A.N., I.S., D.M.-G., P.J., M.P., C.R., F.N., L. Conde, M.J., P.V., L.D.C., D.A.P., M.L.-G., A. Moros, G.R., L. Colomo, A. Martínez, A.V., J.I.M.-S., V.A., L.H., A.E., R.S., and E.C. performed research; P.V., L.D.C., M.A., P.F., A. Muntañola, E.M.H., A.R., G.O., J.M.H.-R., W.K., R.S., A.W., W.H.W., and D.C. contributed new reagents/analytic tools; S.B., R.V.-M., A.N., I.S., D.M.-G., P.J., E.G., M.P., C.R., M.J., G.C., G.R., N.V., J.I.M.-S., M.R., M.J.C., R.S., D.C., A.L.-G., C.L.-O., X.S.P., and E.C. analyzed data; and S.B., C.L.-O., X.S.P., and E.C. wrote the paper.

The authors declare no conflict of interest.

*This Direct Submission article had a prearranged editor.

Freely available online through the PNAS open access option.

Data deposition: Next-generation sequencing data have been deposited at the European Genome-Phenome Archive under accession no. EGAS00001000510. Affymetrix SNP6.0 array and HU133+2.0 gene expression data have been deposited at Gene Expression Omnibus (GEO) under accession nos. GSE46969 and GSE36000, respectively.

[1]To whom correspondence may be addressed. E-mail: ecampo@clinic.ub.es, sbea@clinic.ub.es, or xspuente@uniovi.es.

[2]C.L.-O., X.S.P., and E.C. contributed equally to this work.

This article contains supporting information online at www.pnas.org/lookup/suppl/doi:10.1073/pnas.1314608110/-/DCSupplemental.

addition, we performed WES of six MCL cell lines. Selected mutated genes were investigated in a validation series of 172 MCL patients (*SI Appendix*, Tables S1–S6). We detected about 3,700 somatic mutations per tumor (1.2 per Mb) by WGS (*SI Appendix*, Figs. S1*A* and S2*A* and Dataset S1). The most common substitution was the transition C > T/G > A, usually occurring in a CpG context. Two *IGHV*-mutated MCL showed a higher proportion of A > C/T > G mutations than the two *IGHV*-unmutated cases (*SI Appendix*, Fig. S1*B*). The breakpoints of the t(11;14) translocation differed in the four cases (13) (*SI Appendix*, Table S7). We next investigated the presence of regional clustering of somatic mutations by constructing "rainfall plots" (*SI Appendix*, Fig. S2*B*). Foci of hypermutation or *kataegis*, a phenomenon recently described in breast cancer (14), were observed in three cases. They were more frequent in the two *IGHV*-mutated tumors. These clusters occurred around the 11q13 breakpoint of the t(11;14); the Ig genes at 2p11, 14q32.33, and 22q11.22; and the deleted 9p21.3 region, but we also observed this phenomenon in regions without apparent structural alterations and lacking coding genes (*SI Appendix*, Table S8). The same clusters of hypermutation were observed in the sequential sample of case M003, suggesting that *kataegis* in MCL may occur as an early phenomenon that remains stable during the evolution of the disease.

We further characterized the spectrum of mutations in 29 MCL by WES (*SI Appendix*, Tables S1, S3, and S9 and Dataset S2). All these cases were also analyzed by SNP array for copy number alterations (CNA) and copy number neutral loss of heterozygosity (*SI Appendix*, Fig. S3 and Table S10). We identified 652 protein-coding genes with somatic mutations affecting the structure of the encoded protein (nonsynonymous changes, frameshifts in the coding sequence, and mutations affecting canonical splicing sites) with a median of 20 mutations per case (range 8–47). Twenty-five of the 33 mutated genes in at least two samples were mutated at a rate significantly higher than expected by chance, and all tumors harbored mutations in at least 1 of these 25 genes (Fig. 1 and *SI Appendix*, Table S11). Similarly, five of the six MCL cell lines also had mutations in at least one of the recurrently mutated genes identified in primary tumors (Fig. 1, *SI Appendix*, and Dataset S3). Chromosomal CNAs were present in 26/29 (90%) cases (mean 11.1 ± 9.2 per altered case) (*SI Appendix*, Fig. S3 and Table S10). Tumors expressing *SOX11* showed a significantly higher number of CNAs than SOX11-negative MCLs (mean 13 ± 9 versus 2 ± 2; $P = 2.1 \times 10^{-5}$), despite the similar number of somatic mutations (mean 24 ± 12 versus 17 ± 9; $P = 0.141$) (Fig. 1). Interestingly, five patients who did not need treatment (median 55 mo, range 4–147) had significantly fewer somatic protein-coding mutations (mean 11 ± 4 versus 25 ± 11, $P = 3.4 \times 10^{-5}$) and CNAs (mean 2 ± 3 versus 12 ± 9; $P = 0.001$) than patients who required treatment at diagnosis ($n = 24$).

Recurrent Somatic Mutations in MCL. *ATM*, *CCND1*, and *TP53*, previously described as drivers in MCL, were among the most frequently mutated genes in this study. *ATM* mutations were found in 12 of the 22 (55%) tumors expressing *SOX11*, but in none of the SOX11-negative MCL ($P = 0.023$) (Table 1, Fig. 1, and *SI Appendix*, Table S9). Six of the mutations were associated with deletions of the wild-type allele, whereas five cases with no 11q loss had two different *ATM* mutations per case and only one was a single mutation with no 11q deletion (*SI Appendix*, Fig. S4*A*). These mutations mainly truncated or affected functional domains (*SI Appendix*, Fig. S5). *CCND1* mutations were found predominantly in exon 1 (9 of 10 *CCND1*-mutated cases) (*SI Appendix*, Fig. S6) and were more frequent in SOX11-negative MCL [6/7 (86%) versus 4/22 (18%); $P = 0.03$] and with *IGHV*-mutated [7/12 (58%) versus 3/16 (19%), $P = 0.05$], suggesting their acquisition in the germinal center microenvironment (Fig. 1, Table 1, and *SI Appendix*, Table S9). *TP53* mutations [8/29 (28%)] were associated with 17p alterations in six cases, and only one case without 17p alteration had two mutations. *TP53*

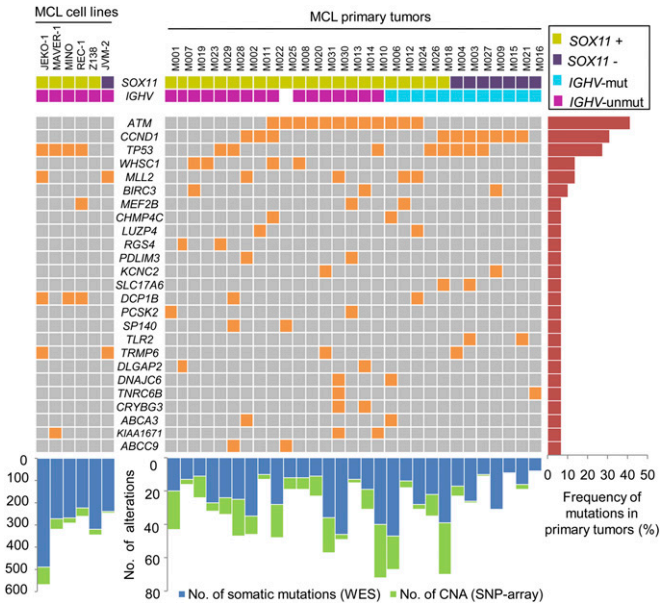

Fig. 1. WES in 29 cases and 6 MCL cell lines. Heatmap with the mutation pattern of the 25 significantly recurrent mutated genes. Each row represents a gene and each column represents a primary tumor/cell line. Vertical bar graphs show the total number of somatic mutations by WES (blue) and somatic CNAs by SNP array (green) for primary tumors, and the total number of nonpolymorphic variants and CNAs for cell lines. The plot below the case label indicates sample characteristics (*SOX11* expression and *IGHV* gene status).

mutations were equally distributed in tumors regardless of *SOX11* expression or *IGHV* mutations (Fig. 1).

We also identified recurrent mutations in *WHSC1*, *MLL2*, *BIRC3*, *MEF2B*, and *TLR2* (Table 1; Fig. 1), as well as *NOTCH2* in one case. *WHSC1* encodes a histone 3 methyltransferase of lysine-36 (H3K36) that has not been found previously mutated in lymphomas. Two missense mutations (p.E1099K and p.T1150A) were recurrently found in two cases each. Both residues are in close proximity and affect two of the most conserved domains in exons 18 and 19. We further analyzed these exons in 101 additional tumors and confirmed the presence of the same mutations in nine more cases [total 13/130 (10%)] (Table 1, Fig. 2*A*, and *SI Appendix*, Table S9 and Fig. S7). Interestingly, *WHSC1* (also named *MMSET* or *NSD2*) is the target of the *IGH*-translocation t(4;14) in plasma cell myeloma (PCM), where it is overexpressed and associated with an increase in H3K36 and a decrease in H3K27 methylation across the genome (15). Gene expression analysis of 8 *WHSC1*-mutated and 31 *WHSC1*-unmutated MCL identified 236 genes differentially expressed (false discovery rate <5%) with the majority of these genes [192/236 (81%)] up-regulated in the *WHSC1*-mutated cases (Fig. 3*B*; *SI Appendix*, Table S12). A gene set enrichment analysis (GSEA) using previously published lymphoid gene expression signatures (15) demonstrated that *WHSC1*-mutated cases displayed significant overexpression of several signatures related to proliferation and cell-cycle regulation (*SI Appendix*, Fig. S8) (16). Interestingly, *WHSC1*-mutated MCL showed a highly significant overexpression of the gene signature up-regulated in PCM with the t(4;14) translocation overexpressing *WHSC1* (17). In addition, *WHSC1*-mutated MCL showed overexpression of genes up-regulated by wild-type *WHSC1* or the gain-of-function exon 19 mutant *WHSC1* in the KMS11 PCM cell line (15) (*SI Appendix*, Fig. S8).

In addition, the histone methyltransferase *MLL2* was mutated in 4/29 primary tumors and 2/6 MCL cell lines. Four of the six mutations were truncating and two were missense changes and affected the conserved FYRN and FYRC domains (Table 1 and *SI Appendix*, Fig. S9). None of these cases had a deletion of the

Table 1. Frequency of recurrently mutated genes in mantle cell lymphoma

Gene	Cell lines	MCL cases, %	SOX11+ MCL, %	*IGHV*-U MCL, %
ATM		41 (12/29)	55 (12/22)*	50 (8/16)
CCND1		35 (10/29)	18 (4/22)*	19 (3/16)*
MLL2	2/9	14 (4/29)	18 (4/22)	13 (2/16)
WHSC1		10 (13/130)	15 (12/82)*	14 (11/80)
BIRC3		6 (11/173)	7 (7/95)	9 (9/97)
NOTCH2		5 (9/172)	6 (6/93)	6 (6/95)
NOTCH1	2/9	5 (8/172)	5 (5/95)	7 (7/95)
MEF2B	1/9	3 (6/187)	5 (5/100)	4 (4/102)
TLR2		1 (2/171)	0/94	0/96

Data are from WES and Sanger sequencing. *IGHV*-U, *IGHV*-unmutated gene.
*Significant *P* values (see details in *SI Appendix*, Table S9).

second allele. *MEF2B* carried the same p.K23R somatic mutation in exon 2 in 2/29 primary tumors, and a p.N49S mutation in exon 2 was found in the REC-1 cell line. We then expanded the study of exon 2 in 158 MCL cases and found the same p.K23R mutation in four additional tumors [total 6/187 (3.2%)] (Table 1 and *SI Appendix*, Figs. S7 and S10).Virtually all *WHSC1*, *MLL2*, and *MEF2B* mutations occurred in MCL expressing SOX11.

Deletions of 11q21–q23 are common alterations in MCL. In addition to *ATM*, *BIRC3* is also located in this region (11q22.2). We found inactivating mutations in exon 9 in two MCL cases and a splice-site mutation in an additional patient (Table 1, Fig. 1, and Fig. 3*C*). We expanded the study and found mutations in 11/173 (6.4%) cases, and these cases had more frequent 11q deletions than *BIRC3*-unmutated MCL [10/11 (91%) versus 25/87 (29%), respectively; $P = 1.1 \times 10^{-4}$] (Fig. 2*D*).

We found two mutations of *TLR2* in two SOX11-negative/*IGHV*-mutated MCL (Table 1). One of these mutations (p.D327V) had been previously identified in one *IGHV*-mutated chronic lymphocytic leukemia (CLL) (18). To determine the potential functional activity of these mutations, we stimulated primary cells of the two *TLR2*-mutated MCL cases (M021, M003), the mutated CLL case, and 11 unmutated controls (3 CLL, 4 MCL, and 4 normal B-cell samples) with TLR2 agonists and assessed the response of 25 cytokines. CLL and MCL cells carrying the p.D327V mutation showed a significant increased secretion of IL-1RA and IL-6 and, to a lesser extent, of IL-8 compared with *TLR2*-unmutated samples (Fig. 2*E* and *SI Appendix*, Fig. S11). The MCL carrying the p.Y298S mutation had extremely high basal levels of IL-6 compared with the basal or poststimulation levels of other tumors or normal B lymphocytes (Fig. 2*F*). Several TLR2 agonist stimuli (PGN-SA, LTA-SA, or PAM3) did not generate additional IL-6 increases in these cells.

Among the other mutated genes, we found mutations of the ubiquitin ligase *UBR5*, recently described in MCL patients (19), and an inactivating mutation affecting *B2M* (p.L13fs*10) in a MCL carrying a 15q12–q21.1 deletion, encompassing the *B2M* locus. However, we did not find mutations in an additional 97 MCL patients, including 3 with a similar 15q monoallelic deletion.

***NOTCH2* and *NOTCH1* Mutations in MCL.** The finding of a *NOTCH2* mutation prompted us to expand the analysis of the HD, TAD, and PEST domains in additional tumors, and we found mutations in 9/172 MCL (5.2%) (Table 1; Fig. 3*A*). All these mutations generate a premature stop codon within the PEST domain. Gene expression analysis of two *NOTCH2*-mutated and 19 *NOTCH2*-unmutated MCL (also wild-type for *NOTCH1*) showed many differentially expressed genes ($n = 841$) (false discovery rate < 5%); 42% of them ($n = 355$) were up-regulated in *NOTCH2*-mutated cases and were significantly enriched in cell-cycle and metabolic pathways (Fig. 3*B*, *SI Appendix*, and Dataset S4). GSEA showed that *NOTCH2* mutated samples displayed a significant overexpression of genes up-regulated by NOTCH activation in lymphoid cells (20) and also had a concordant modulation of gene signatures regulated by NOTCH inhibition in MCL cell lines (21–23) (*SI Appendix*, Fig. S12). *NOTCH2* mutations occurred more frequently in blastoid/pleomorphic MCL (66 versus 18%, $P = 0.001$) and conferred a dismal prognosis [3-y overall survival (OS): 0 versus 62%, $P = 2.5 \times 10^{-4}$] (Fig. 3*C*). *TP53* mutations were found in 42/192 patients (22%) and were also associated with poor outcome. In a bivariate analysis, both *NOTCH2* mutations (hazard ratio: 3.5; 95% confidence interval: 1.3–9.5; $P = 0.017$) and *TP53* mutations (hazard ratio: 2.4; 95% confidence interval: 1.4–4.2; $P = 0.003$)

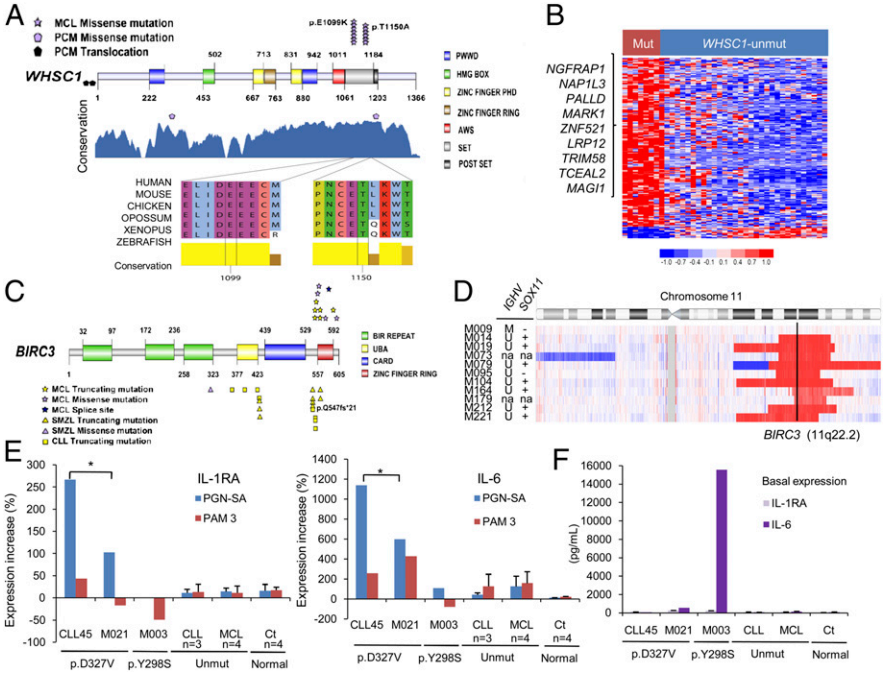

Fig. 2. *WHSC1*, *BIRC3*, and *TLR2* alterations in MCL. (*A*) *WHSC1* mutations in MCL (above gene symbol) and PCM (below gene symbol) (41). Amino acid conservation of *WHSC1* (blue plot), and multiple sequence alignment of the region containing the two mutations in residues E1099 and T1150. (*B*) Heatmap showing the 236 differentially expressed genes in *WHSC1*-mutated versus *WHSC1*-unmutated MCL cases. (*C*) *BIRC3* mutations in MCL (*Upper*) and other hematologic neoplasms (*Lower*) (38, 39, 42). (*D*) Graphic representation of 11q deletions in *BIRC3*-mutated cases. Ten of 11 mutated MCL cases carried deletions encompassing *BIRC3* gene (11q22.2). *(E)* Plots representing cytokine levels secreted by B cells from tumors and healthy donors. Only IL-1RA and IL-6 showed differences between *TLR2*-mutated and -unmutated samples. Percentage of increase or decrease of cytokine expression before and after stimulation with PGN-SA (blue bars) and PAM3 (red bars). *Significance comparing the two cases with p.D327V mutation versus *TLR2*-unmutated tumors ($P = 0.037$ and 0.026 for IL-1RA and IL-6, respectively). *(F)* Basal levels of IL-6 and IL-1RA in MCL, CLL, and normal B cells.

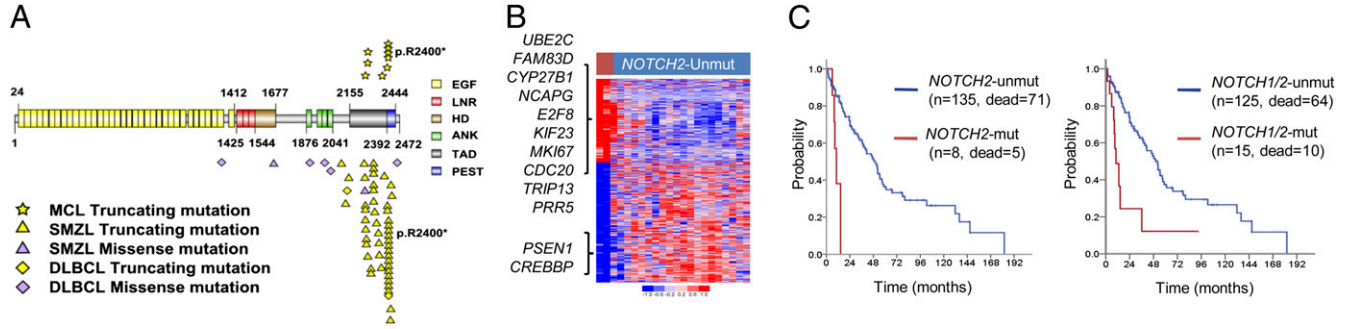

Fig. 3. *NOTCH2* alterations in mantle cell lymphoma. (*A*) *NOTCH2* mutations in MCL (*Upper*) and other hematologic neoplasms (*Lower*) (37, 38, 43). (*B*) Heatmap showing the 841 differentially expressed genes in *NOTCH2*-mutated versus *NOTCH2*-unmutated MCL cases. (*C*) Actuarial probability of overall survival of MCL patients according to *NOTCH2* mutation and *NOTCH2* or *NOTCH1* mutation.

were identified as independent risk factors for OS (*SI Appendix*, Fig. S13).

NOTCH1 mutations have been recently described in MCL (20). We investigated this gene and found truncating mutations in 8/172 (4.6%) MCL cases, as well as in MINO and REC-1 cells (Table 1 and *SI Appendix*, Fig. S14). *NOTCH1*-mutated tumors were predominantly blastoid/pleomorphic (67 versus 19%, $P = 0.03$) and showed shorter survival than *NOTCH1*-unmutated MCL (3-y OS: 33 versus 60%, $P = 0.026$) (*SI Appendix*, Fig. S15). *NOTCH1* and *NOTCH2* mutations occurred in different subsets of tumors because only 1 of the 16 patients with mutations in these genes had mutations in both. Taken together, *NOTCH1/2* mutations were present in 9.5% of MCL and identified a subset of tumors with more adverse biological and clinical features including blastoid/pleomorphic morphology (67 versus 13%, $P = 1.3 \times 10^{-5}$) and a significant shorter survival (3-y OS: 24 versus 63%, $P = 3.4 \times 10^{-4}$) (Fig. 3*C*).

Sequencing Simultaneous and Subsequent MCL Samples Reveals Clonal Heterogeneity. To explore the subclonal architecture of MCL, we sequenced a second tumor sample obtained simultaneously from two different topographic sites ($n = 6$) or at two time points (diagnosis and disease progression, $n = 2$). Analysis of the frequency of reads supporting somatic substitution allowed the estimation of major subclonal populations (24). Four of the six patients with simultaneous samples showed the same mutations and CNAs in the peripheral blood (PB) sample and corresponding lymphoid tissue, suggesting the presence of a single major clone at both sites. In contrast, two cases (M023 and M026) had a subset of common mutations in both topographic sites, but they also carried a subset of mutated genes that were exclusive of the PB or tissue tumor sample (Fig. 4 *A* and *B*). This pattern of alterations is consistent with two major subpopulations derived from an initial founder clone differentially represented in the two topographic sites. In addition, we also observed a different pattern of genomic alterations at diagnosis and progression in the two cases with sequential samples (Fig. 4*C* and *D* and *SI Appendix*, Table S10). Patient M003 had stable disease without treatment for more than 3 y and then rapidly progressed. The major clone identified at diagnosis gained new mutations and genomic complexity at the time of clinical progression. This new clone carried the same 17p deletion and somatic mutations observed in the initial sample, but had a 16% increase in the number of whole-genome mutations (from 3,928 to 4,665) (*SI Appendix*, Fig. S1*A*). These included nonsynonymous mutations in additional genes, a complex DNA copy number profile with 20 acquired CNAs, and chromothripsis involving chromosomes 4 and 12 (Fig. 4*C* and *SI Appendix*, Fig. S2*A*). Patient M002 was treated with chemotherapy after diagnosis and relapsed 3 y later. The major clone at relapse maintained a subset of CNAs and somatic mutations present at diagnosis, but 11 of the initial mutations had disappeared and other mutated genes had emerged (Fig. 4*D*). This pattern of evolution is consistent with the eradication of the major initial subclone by chemotherapy and the relapse of a new subclone after treatment.

Comparison of the allele frequency of mutations in the different simultaneous or evolving subclones may help to infer the dynamic architecture of somatic events in the evolution of tumors (24, 25). Eight of the 25 recurrently mutated genes in MCL (*ATM*, *CCND1*, *MLL2*, *KCNC2*, *KIAA1671*, *PCSK2*, *TNRC6B*, and *TRPM6*) were present at similar allelic frequency in the two subclones of different cases, suggesting that they represent early events. In contrast, four recurrently mutated genes (*ABCA3*, *TLR2*, *TP53*, and *WHSC1*) were seen in only one of the two simultaneous or emerging subclones at progression, supporting the notion that they might constitute later events. We further analyzed by Sanger sequencing 11 additional serial and 8 simultaneous tumor samples from different topographic sites (PB and lymphoid tissues) (*SI Appendix*, Fig. S16). Interestingly, we observed that *BIRC3* mutations were absent at diagnosis in two cases that acquired the mutation in a posttreatment sample associated with the acquisition of an 11q22.1–q24.2 deletion in one of them. Another case showed the *BIRC3* mutation in the PB but not in the simultaneous lymph node. Additionally, *NOTCH1* was mutated in only one of the synchronic samples in two cases.

Discussion

We have conducted a comprehensive genomic study of MCL that has revealed the heterogeneous spectrum of somatic mutations of this tumor, with several molecular mechanisms contributing to the pathogenesis and the clinical progression of the disease. The genome sequencing of simultaneous and sequential tumor samples has highlighted the subclonal heterogeneity of the mutations already present at diagnosis and their dynamic evolution in the progression of the disease.

The whole-genome analysis showed a relative low number of global somatic mutations in MCL (1.2 per Mb), slightly higher to CLL (26) or acute myeloid leukemia (27), but lower than in other lymphoid or nonhematopoietic tumors (28, 29). Interestingly, we identified a distinct mutational signature characterized by A > C/T > G substitutions in a TpA context in the two MCL with *IGHV*-mutated. This signature was initially identified in CLL with *IGHV*-mutated and more recently confirmed as a unique feature of lymphoid neoplasms originating in germinal center cells (26, 29) and has been attributed to the action of the error-prone DNA polymerase η during the *IGHV* somatic hypermutation process (26).

The most commonly mutated genes were the previously identified MCL drivers *ATM*, *CCND1*, and *TP53*. These mutations were differentially distributed in subtypes of the disease according to the *IGHV* mutational status and SOX11 expression. Thus, *ATM* mutations were seen only in SOX11-positive tumors, whereas *CCND1* mutations were preferentially detected in MCL with *IGHV*-mutated and *TP53* mutations were equally

MEDICAL SCIENCES

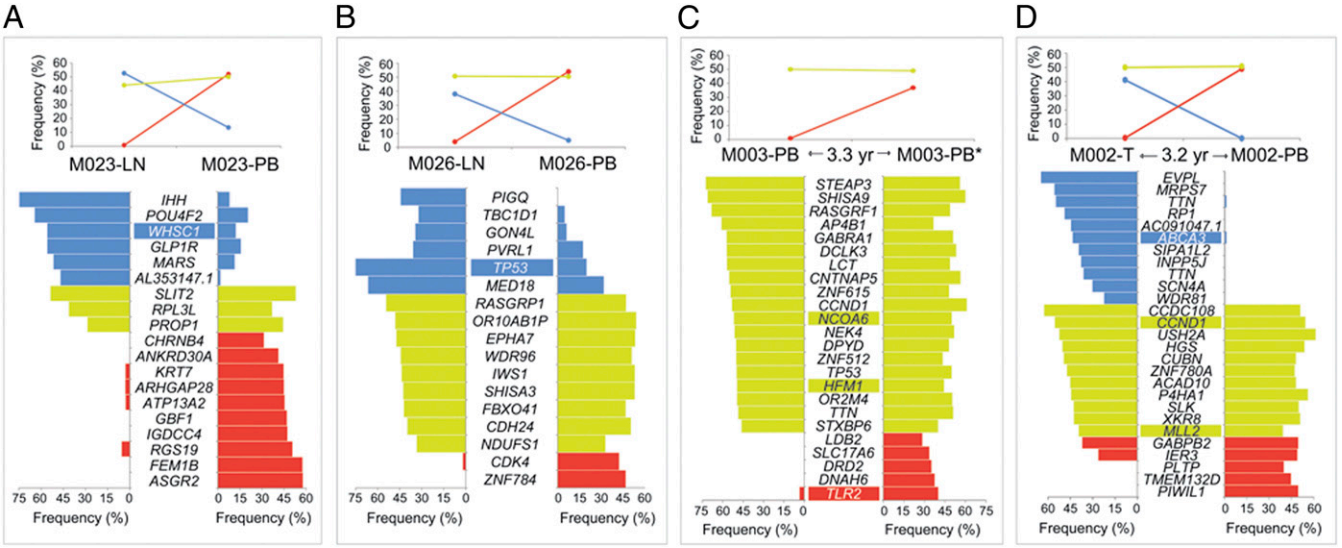

Fig. 4. Subclonal architecture in MCL. Representation of four informative MCL patients with two tumor samples analyzed. The mutation clusters are represented in the upper panel of each case, the shared and stable mutations are in green color, in blue the mutations specific of the first sample and in red the mutations identified only in the second sample. In the lower panel of each case, a detailed representation of the percentage of mutated reads in each of the samples (*Left* and *Right*) with the same color code, and with the significantly recurrent mutated genes highlighted in the same color. (*A–B*) Cases M023 and M026 have two major subclones derived from an initial founder clone differentially represented in simultaneous samples of lymph node (LN) and peripheral blood (PB). (*C*) Longitudinal analysis in patient M003 at diagnosis and at disease progression previous to treatment. (*D*) Longitudinal analysis in patient M002 at diagnosis and at first relapse.

distributed among the different groups. The integration of the CNA and somatic mutations showed that only *TP53*, *ATM*, and *BIRC3* recurrent mutations were associated with allelic losses (17p and 11q, respectively), whereas *CDKN2A*, the only gene targeted by recurrent homozygous deletions, did not carry somatic mutations in other cases. Interestingly, three mutated genes (*WHSC1, MLL2*, and *MEF2B*) function as chromatin modifiers, and altogether these mutations occurred in 10 of the 29 (14%) cases examined by WES. The analysis of *WHSC1* and *MEF2B* in an expanded series confirmed the relative high frequency of these mutations in MCL (10% and 3.2%, respectively). *WHSC1* mutations have not been described previously in lymphomas, but this gene is the target of the t(4;14) translocation in PCM, and the same mutation observed in exon 18 has been recently detected in an acute lymphoblastic leukemia (ALL) patient (30). The *WHSC1* overexpression in PCM and the mutation in ALL seem to have an activating function because they increase the H3K36 methylation associated with a methylation decrease in H3K27 across the genome (15). Our *WHSC1*-mutated primary MCL had the same overexpressed gene signatures modulated by *WHSC1* activation in PCM, suggesting that these mutations may also have a similar activating function in MCL. The mutations observed in *MLL2* and *MEF2B* are similar to those detected in diffuse large B-cell lymphoma (DLBCL) and follicular lymphomas, but their functional consequences are not yet well understood (31–33). Notably, virtually all *MLL2*, *WHSC1*, and *MEF2B* mutations were found in MCL with *IGHV*-unmutated or expressing SOX11.

Recent studies have suggested a role of microenvironment stimuli in sustaining MCL (1). *TLR*s mediate cell responses to specific pathogen-associated molecular patterns (34). In that sense, we found mutations of *TLR2* in two SOX11-negative/*IGHV*-mutated MCL, and these mutations were associated with increased production of IL-1RA and IL-6 by the tumor cells. Notably, high levels of IL-1RA have been associated with aggressive behavior in some lymphomas (35), and IL-6 sustains growth and survival of MCL cells (36). These findings suggest that *TLR2* mutations may contribute to the pathogenesis of a subset of SOX11-negative/*IGHV*-mutated MCL by modulating tumor microenvironment responses.

In addition to the statistically significant mutations described above, we found a mutation in *NOTCH2* in one MCL. Similar activating mutations have been recently described in splenic marginal zone lymphomas and in *NOTCH1* in aggressive CLL and MCL (37, 38). These findings prompted us to expand the study of *NOTCH2* and *NOTCH1* mutations in MCL and found their presence in 5.2% and 4.7% of the tumors, respectively. All these mutations generated truncating and likely more active proteins and occurred in a subset of tumors with very aggressive clinical behavior. Only 1 of 16 tumors had simultaneous mutations in both genes, suggesting that they may give a similar selective advantage to the cells. All these findings indicate that *NOTCH1/2* mutations in MCL activate this pathway and are a frequent mechanism involved in the aggressive behavior of the tumors.

The spectrum of mutations described in this work highlights the existence of common molecular features as well as relevant differences in the genetic alterations present in different subtypes of lymphoid neoplasms. Thus, *NOTCH1* mutations have been found in CLL (18, 26) whereas *NOTCH2* is mutated in splenic marginal zone lymphomas (37, 38); however, none of these tumors carry mutations in both *NOTCH* genes as observed in MCL. In addition, *MLL2* and *MEF2B* mutations are shared with DLBCL (31–33) but are uncommon in CLL, whereas MCL has frequent mutations of *ATM* and *BIRC3* that are also frequent in CLL (39) but uncommon in DLBCL. In contrast, *WHSC1* mutations appear to be specific for MCL while lacking mutations in genes frequently mutated in other hematological neoplasias (e.g., *MYD88*, *CARD11*, *EZH2*, *SF3B1*).

Recent genomic studies have revealed the complex subclonal heterogeneity of different tumors and its dynamic evolution in the course of the disease (40). The sequence of two simultaneous or longitudinal samples in different topographic sites in our study has revealed that some tumors may have at least two major subclones already at diagnosis with different representation in two topographic sites, lymph nodes, and peripheral blood. In addition, the evolution of the tumors is also heterogeneous with the eradication of some clones by the chemotherapy treatment and the emergency of other new clones at the progression of the disease or at relapse after chemotherapy. The analysis of the

allelic frequency of the mutations allows the recognition of initial and acquired mutations that are probably relevant in the progression of the disease (24, 25). The recognition of this molecular heterogeneity at diagnosis and progression may have future clinical relevance for the management of patients with targeted therapies to specific mutations.

In summary, this whole-genome/whole-exome study of MCL has revealed genes and pathways recurrently mutated that may contribute to lymphomagenesis in cooperation with the t(11;14) translocation. The differential distribution of these mutations in clinical and molecular subtypes of the disease illustrates the relationship between genomic alterations and tumor heterogeneity. We have also shown the intratumoral heterogeneity and subclonal architecture of MCL that may have relevance in the clinical evolution of the tumors. These alterations highlight mechanisms in the pathogenesis of this lymphoma and offer potential targets for therapeutic intervention.

Materials and Methods

Patients and Specimens. We sequenced the genomes of 29 patients with MCL and six MCL cell lines. Additional samples from 172 patients were obtained for clinical validation. All patients gave informed consent for sample collection and analysis. DNA and RNA were purified from tumors and normal cells. Additional details are provided in *SI Appendix, SI Materials and Methods*.

Whole-Genome and Whole-Exome Sequencing and Analysis. Whole-genome and whole-exome sequencing (Agilent SureSelect Human All Exon 50 MB) were performed as previously described (18, 26) using a HiSeq 2000 instrument. Sequence data analysis was performed using the Sidrón mutation caller as described (18, 26). Additional details are provided in *SI Appendix, SI Materials and Methods*.

Microarray Experiments. Genotyping and copy number and gene expression analysis were performed using Affymetrix SNP6.0 arrays and HU133+ 2.0 GeneChip (Affymetrix), respectively. Additional details are provided in *SI Appendix, SI Materials and Methods*.

ACKNOWLEDGMENTS. We thank M. Prieto, S. Guijarro, M. Sánchez, L. Pla, S. Martín, C. Capdevila, N. de Moner, N. Villahoz, and C. Muro for their assistance; and the Spanish Centro Nacional de Análisis Genómico, Centro Nacional de Genotipado, and Institut d'Investigacions Biomèdiques August Pi i Sunyer Genomic Unit for their services. This work was developed at the Centro Esther Koplowitz, Barcelona, Spain, and supported by the Fondo de Investigaciones Sanitarias (PI11/01177, PI10/01404); Association for International Cancer Research (12-0142); Lymphoma Research Foundation; Red Temática de Investigación Cooperativa en Cáncer (RD06/0020/0039; RD12/0036/0036); Plan Nacional (SAF08/03630, SAF10/21165, SAF12/38432); Generalitat de Catalunya 2009-SGR-992; and the European Regional Development Fund. C.L-O. is a Botín Foundation investigator and E.C. is an Institució Catalana de Recerca i Estudis Avançats-Academia investigator. A.W. and W.H.W. are supported by the intramural research program of National Heart, Lung, and Blood Institute and National Cancer Institute, respectively.

1. Jares P, Colomer D, Campo E (2012) Molecular pathogenesis of mantle cell lymphoma. *J Clin Invest* 122(10):3416–3423.
2. Gladden AB, Woolery R, Aggarwal P, Wasik MA, Diehl JA (2006) Expression of constitutively nuclear cyclin D1 in murine lymphocytes induces B-cell lymphoma. *Oncogene* 25(7):998–1007.
3. Beà S, et al. (2009) Uniparental disomies, homozygous deletions, amplifications, and target genes in mantle cell lymphoma revealed by integrative high-resolution whole-genome profiling. *Blood* 113(13):3059–3069.
4. Rosenwald A, et al. (2003) The proliferation gene expression signature is a quantitative integrator of oncogenic events that predicts survival in mantle cell lymphoma. *Cancer Cell* 3(2):185–197.
5. Vose JM (2012) Mantle cell lymphoma: 2012 update on diagnosis, risk-stratification, and clinical management. *Am J Hematol* 87(6):604–609.
6. Martin P, et al. (2009) Outcome of deferred initial therapy in mantle-cell lymphoma. *J Clin Oncol* 27(8):1209–1213.
7. Fernàndez V, et al. (2010) Genomic and gene expression profiling defines indolent forms of mantle cell lymphoma. *Cancer Res* 70(4):1408–1418.
8. Orchard J, et al. (2003) A subset of t(11;14) lymphoma with mantle cell features displays mutated IgVH genes and includes patients with good prognosis, nonnodal disease. *Blood* 101(12):4975–4981.
9. Navarro A, et al. (2012) Molecular subsets of mantle cell lymphoma defined by the IGHV mutational status and SOX11 expression have distinct biologic and clinical features. *Cancer Res* 72(20):5307–5316.
10. Ondrejka SL, Lai R, Smith SD, Hsi ED (2011) Indolent mantle cell leukemia: A clinicopathological variant characterized by isolated lymphocytosis, interstitial bone marrow involvement, kappa light chain restriction, and good prognosis. *Haematologica* 96(8):1121–1127.
11. Royo C, et al. (2012) Non-nodal type of mantle cell lymphoma is a specific biological and clinical subgroup of the disease. *Leukemia* 26(8):1895–1898.
12. Vegliante MC, et al. (2013) SOX11 regulates PAX5 expression and blocks terminal B-cell differentiation in aggressive mantle cell lymphoma. *Blood* 121(12):2175–2185.
13. Greisman HA, et al. (2012) IgH partner breakpoint sequences provide evidence that AID initiates t(11;14) and t(8;14) chromosomal breaks in mantle cell and Burkitt lymphomas. *Blood* 120(14):2864–2867.
14. Nik-Zainal S, et al.; Breast Cancer Working Group of the International Cancer Genome Consortium (2012) Mutational processes molding the genomes of 21 breast cancers. *Cell* 149(5):979–993.
15. Martinez-Garcia E, et al. (2011) The MMSET histone methyl transferase switches global histone methylation and alters gene expression in t(4;14) multiple myeloma cells. *Blood* 117(1):211–220.
16. Shaffer AL, et al. (2006) A library of gene expression signatures to illuminate normal and pathological lymphoid biology. *Immunol Rev* 210(1):67–85.
17. Zhan F, et al. (2006) The molecular classification of multiple myeloma. *Blood* 108(6): 2020–2028.
18. Quesada V, et al. (2012) Exome sequencing identifies recurrent mutations of the splicing factor SF3B1 gene in chronic lymphocytic leukemia. *Nat Genet* 44(1):47–52.
19. Meissner B, et al. (2013) The E3 ubiquitin ligase UBR5 is recurrently mutated in mantle cell lymphoma. *Blood* 121(16):3161–3164.
20. Kridel R, et al. (2012) Whole transcriptome sequencing reveals recurrent NOTCH1 mutations in mantle cell lymphoma. *Blood* 119(9):1963–1971.
21. Palomero T, et al. (2006) NOTCH1 directly regulates c-MYC and activates a feed-forward-loop transcriptional network promoting leukemic cell growth. *Proc Natl Acad Sci USA* 103(48):18261–18266.
22. Sharma VM, et al. (2006) Notch1 contributes to mouse T-cell leukemia by directly inducing the expression of c-myc. *Mol Cell Biol* 26(21):8022–8031.
23. Weng AP, et al. (2004) Activating mutations of NOTCH1 in human T cell acute lymphoblastic leukemia. *Science* 306(5694):269–271.
24. Landau DA, et al. (2013) Evolution and impact of subclonal mutations in chronic lymphocytic leukemia. *Cell* 152(4):714–726.
25. Puente XS, López-Otín C (2013) The evolutionary biography of chronic lymphocytic leukemia. *Nat Genet* 45(3):229–231.
26. Puente XS, et al. (2011) Whole-genome sequencing identifies recurrent mutations in chronic lymphocytic leukaemia. *Nature* 475(7354):101–105.
27. Ley TJ, et al. (2010) DNMT3A mutations in acute myeloid leukemia. *N Engl J Med* 363(25):2424–2433.
28. Lawrence MS, et al. (2013) Mutational heterogeneity in cancer and the search for new cancer-associated genes. *Nature* 499(7457):214–218.
29. Alexandrov LB, et al. (2013) Signatures of mutational processes in human cancer. *Nature* 500(7463):415–421.
30. Oyer JA, et al. (2013) Point mutation E1099K in MMSET/NSD2 enhances its methyltranferase activity and leads to altered global chromatin methylation in lymphoid malignancies. *Leukemia*, 10.1038/leu.2013.204.
31. Morin RD, et al. (2011) Frequent mutation of histone-modifying genes in non-Hodgkin lymphoma. *Nature* 476(7360):298–303.
32. Pasqualucci L, et al. (2011) Analysis of the coding genome of diffuse large B-cell lymphoma. *Nat Genet* 43(9):830–837.
33. Lohr JG, et al. (2012) Discovery and prioritization of somatic mutations in diffuse large B-cell lymphoma (DLBCL) by whole-exome sequencing. *Proc Natl Acad Sci USA* 109(10):3879–3884.
34. Chiron D, Bekeredjian-Ding I, Pellat-Deceunynck C, Bataille R, Jego G (2008) Toll-like receptors: Lessons to learn from normal and malignant human B cells. *Blood* 112(6): 2205–2213.
35. Charbonneau B, et al. (2012) Pretreatment circulating serum cytokines associated with follicular and diffuse large B-cell lymphoma: A clinic-based case-control study. *Cytokine* 60(3):882–889.
36. Zhang L, et al. (2012) Role of the microenvironment in mantle cell lymphoma: IL-6 is an important survival factor for the tumor cells. *Blood* 120(18):3783–3792.
37. Kiel MJ, et al. (2012) Whole-genome sequencing identifies recurrent somatic NOTCH2 mutations in splenic marginal zone lymphoma. *J Exp Med* 209(9):1553–1565.
38. Rossi D, et al. (2012) The coding genome of splenic marginal zone lymphoma: Activation of NOTCH2 and other pathways regulating marginal zone development. *J Exp Med* 209(9):1537–1551.
39. Rossi D, et al. (2012) Disruption of BIRC3 associates with fludarabine chemorefractoriness in TP53 wild-type chronic lymphocytic leukemia. *Blood* 119(12):2854–2862.
40. Gerlinger M, et al. (2012) Intratumor heterogeneity and branched evolution revealed by multiregion sequencing. *N Engl J Med* 366(10):883–892.
41. Chapman MA, et al. (2011) Initial genome sequencing and analysis of multiple myeloma. *Nature* 471(7339):467–472.
42. Rossi D, et al. (2011) Alteration of BIRC3 and multiple other NF-κB pathway genes in splenic marginal zone lymphoma. *Blood* 118(18):4930–4934.
43. Zhang J, et al. (2013) Genetic heterogeneity of diffuse large B-cell lymphoma. *Proc Natl Acad Sci USA* 110(4):1398–1403.